Optimal Trajectory Generation for a Robotic Worm via Parameterization by B-Spline Curves

Mohammad-Reza Sayyed Noorani, Pouya Nourfar

Department of Mechatronic EngineeringUniversity of Tabriz,Tabriz, Iran

smrs.noorani@tabrizu.ac.ir

Department of Mechatronic Engineering Ahar branch - Islamic Azad University Ahar, Iran

pouya.nourfar@gmail.com

Abstract

In this paper we intend to generate some set of optimal trajectories according to the number of control points has been applied for parameterizing those using B-spline curves. The trajectories are used to generate an optimal locomotion gait in a crawling worm-like robot. Due to gait design considerations it is desired to minimize the required torques in a cycle of gait. Similar to caterpillars, progress in our crawling robot is achieved by propagating a trapezoidal wave from tail to head in the vertical plane. According to this model, the optimization problem has been solved via parameterization of joint trajectories, and consequently cost function, using cubic B-spline curves versus variant numbers of control points (CPs) needed in building those. Indeed, it is tried to find the best number of the CPs, of which the cost function obtains a minimum dynamical effort. To this end, the Genetic Algorithm is employed to find the minimal cost value once a nominated number of CPs is considered. Furthermore, since a complete period of this locomotion gait is composed of separated stages called sub-motions, thus the optimal trajectories for each sub-motion is examined independently. The results show choosing the number of CPs between 8 to 12 points constructs the optimized trajectories that reduce the dynamical effort of crawl in comparison with ones are reported by previous researches.

Keywords : Worm-like Robot, B-spline Curves, Optimization, Genetic Algorithm

1- Introduction

Worm-like robot is described as a mono string articulated mechanical device with identical segments that is able to crawl and progress due to a propulsion arising from interaction between its body and the ground, which this is also resulted of propagating a traveling wave through the body from its tail to its head. Recently, worm-like robots that could imitate locomotion pattern of caterpillars have been paid attention by robotic engineers [1-2]. This pattern of crawling is performed in vertical plane in which a trapezoidal-like wave is propagated through the body and lifts some segments of

it up alternatively. Hence, frictional losses and wearing due to traction of the body on the ground become the least. This feature, besides of excellent stability and flexibility that are general features of the crawling locomotion, has caused the increase of interesting in design and realization caterpillar-like locomotion in the robotic inspection devices, especially in order to move in narrow places that are not available for human, e.g. closed pipe lines, or are dangerous for him, e.g. channels of nuclear plants [3-4]. However, capacity of load can be carried by a worm-like robot is low. Particularly, in the case of caterpillar locomotion due to weight of segments of the body lifted up during crawl, there is a less load capacity. Thus, power supply system is embedded in the robot should be lighter, and consequently weaker, which is always a limitation in design of mobile robots, and here is more troublesome. Furthermore, it should also be regarded that size of actuators to be as small as possible for the sake of, first, having the less weight of robot body and second, requiring the less energy to drive the actuators. It is obvious that a smaller actuator produces less torque in identical kinds. This matter imposes the necessity of having a minimum required torque during one cycle of motion in planning the locomotion pattern called "gait generation".

According to this necessity, many efforts have been done in optimal gait generation for variant types of mobile robots [5-6]. A usual method to earn this objective is parameterization of joint trajectories and then looking for parameters constructing the optimal trajectories, minimizing the total required torque if the robot is driven according to those. Moreover, there are various methods for constructing the parametric trajectories. As a superior method for this end, B-spline curves have widely been utilized in optimal trajectory generation. Here, we review some of the recent researches that have employed B-splines for optimal trajectory generation with different applications.

Biagiotti et al. proposed an on-line path planner, in which the sequence of desired via-points should be interpolated along the path, was passed through a FIR filter to computes the control points constructing the B-spline. Then a chain of three moving average filters was used to evaluate the cubic B-spline defined by these control points [7]. Kong et al. presented a novel hybrid cubic B-spline and convex optimization method to solve a time-optimal joint trajectory generation problem with torque and velocity limitations in path coordinate space. Indeed, cubic B-spline was applied to construct a constraint for path smoothness, thereby first and second time derivatives of path coordinate called respectively as pseudo-velocity and pseudo-acceleration, all became continuous and jerk of joints were bounded at the same time [8]. Restrepo et al. exploited the B-spline curves to plan smooth paths for robotic agents to avoid obstacle in a testing environment RoboCup. By using the Kalman filter for predicting the movements of agents, they achieved the optimal control points for B-spline curves [9]. Kang et al. utilized the cubic B-splines for parameterization of active joints

trajectories of biped and quadruped legged robots to determine the energy efficiency of walking and running gaits according to the forward locomotion speed. They presented a formula determines the forward locomotion speed at which running becomes more efficient than walking [10]. Caign et al. presented a feedforward design method for LTI systems as a linear program that optimizes a polynomial B-spline. Indeed, the feedforward signal was formed by a polynomial B-spline. Thus, the optimization method trades off two criteria; first the tracking accuracy as a function of the tracking error between the reference trajectory and output, and second the smoothness of the feedforward signal as a property of the B-spline [11]. Yang, employed B-splines to establish a novel algorithm of Rapidly-exploring Random Tree (RRT) for navigating a mobile robot through cluttered environments, in which both the external and internal constraints of motion have been treated simultaneously. Specially by exploiting the B-spline curves, this algorithm guarantees continuity of curvature along the path by satisfying any upper-bounded curvature constraints [12]. The B-spline functions have even been exploited to model the ocean current flows in which the input variables are latitude, longitude and time, and the output variable is the ocean current velocity in 2D. Thus, this 3D B-spline based model of the ocean current was utilized in establishing a nonlinear trajectory generation algorithm to find the optimal trajectory of an autonomous underwater vehicle (also called glider) [13].

In this paper we intend to utilize a parameterization method based on cubic B-splines to generate optimal trajectories for a worm-like robot having a locomotion gait alike to caterpillars that propagate a vertical trapezoidal-like wave during motion, see Fig 1. In previous works we could step by step approach to this objective by exploiting of optimization methods such as swarm particles optimization [14], and Genetic Algorithm [15]. However, in all of these the parameterization of trajectories was done based on B-splines having 7 control points (CPs) that 4 of them should be fixed to satisfy the boundary conditions. Thus, it is possible that employing the few CPs caused the most optimal trajectories have not been discovered. Hence, objective of this paper is examining variant numbers of CPs in generating the trajectories by B-splines. The genetic algorithm was also utilized as the optimizer.

Fig.1. Natural crawling locomotion of caterpillars, taken from [16]

2- Mathematical Modelling of Worm-Like Robot

A. Locomotion Gait Description

As shown in Fig. 2, a simple locomotion mechanism inspired of caterpillar-mode crawling has been considered that consist of a 5-link planar linkage with revolute joints actuated by servo motors. Advance during a complete cycle of motion is achieved in four separate stages that are called "sub-motions" and indicated by M_1, M_2, M'_2, and M'_1, respectively. By being completed each sub-motion a symmetric trapezoidal loop is pushed forward. Because of being mirror symmetry in the sub-motions, i.e. between M_1 and M_1', and also between M_2 and M_2', it is sufficient considering one sub-motion of each symmetric pair.If α is the maximum of absolute angular displacement of joints,then the joint anglesare reached at the end of each sub-motion, that are the same at the start of the next sub-motion,will be according to Table 1. During performing each sub-motion some links should be remained motionless on the ground until movements of other links are done correctly. In the fact, performing each sub-motion is similar to a planar robotic manipulator having a fixed base, with a main exception that these base links are changed in each sub-motion and thereby move forward during a complete cycle of motion. Being the sufficient friction between the base links and the ground is essential condition for remaining them motionless. Therefore, in deriving the equations of motion for each sub-motion it is assumed this condition is satisfied.Other consideration arises from necessary active actuators in each sub-

motion regarding the degrees of freedom (dof). The sub-motions M_1 and M_2 have three and four dof, respectively. However, it is desired to be tip of the tail or head connected to the ground thoroughly. In other words, it should be held a closed kinematic loop during each sub-motion. Hence, one dof of each sub-motion is reduced. Since we want to minimize the required torque during each sub-motion, and the last link in each sub-motion falls down and closes the loop provided that no torque is applied to its joint, then it is reasonable that the actuator of the last joint in each sub-motion to be passive.

B. Equations of Motion

In order to evaluate the required torque in the sub-motions it is necessary to solve the inverse dynamics problem according to a given nominal trajectories. Thus, the dynamical equations governing in each sub-motion must be available. Those have already been derived in detail, separately, for each sub-motion by [15], and more general by [17]. It is noted that for the sake of convenience only, establishing the equations of motion in each sub-motion has been done using a local coordinate set. Hence,we introduce the below local coordinate sets that are in relation to the global ones shown in Fig. 2.

$$
\begin{aligned}
&\text{in sub-motion } M_1: \\
&\{\theta_1, \theta_2, \theta_3\}^t := \{\theta_2^*, \theta_3^*, \theta_4^*\}^t \\
&\text{in sub-motion } M_2: \\
&\{\theta_1, \theta_2, \theta_3, \theta_4\}^t := \{\theta_1^*, \theta_2^*, \theta_3^*, \theta_4^*\}^t
\end{aligned}
\tag{1}
$$

Since the objective of using the equations of motion is solving the inverse dynamics

problem and not to control, then these were explained in terms of absolute angles of the links,measured with respect to positive direction of horizontal axis, calculated as the below:

$$\varphi_0 = 0, \quad \varphi_i = \varphi_{i-1} + \theta_i, \quad i = 1,...,n \quad (2)$$

Also, the closed loop constraint in each sub-motion can be formulated as the below:

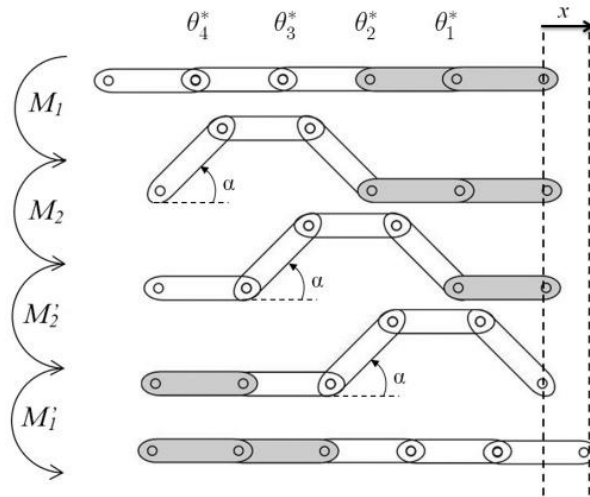$$\sum_{i=1}^{n} \sin \varphi_i = 0 \quad (3)$$

Fig.2.Locomotion mechanism of the caterpillar-mode crawling robot

This constraint equation is used to calculate the passive joint angle in each sub-motion, when the other actuated ones are prescribed. In the other words, the nominated trajectories for actuated joints are acceptable, when those satisfy the constraint equation (3) together with an evaluated real value trajectory for passive joint angle. Thus, the equations of motion governing in sub-motion M_1 has been explained as follows:

$$\frac{ml^2}{6}\begin{pmatrix} 14 & 9\,c_{12} & 3\,c_{13} \\ 9\,c_{12} & 8 & 3\,c_{23} \\ 3\,c_{13} & 3\,c_{23} & 2 \end{pmatrix}\begin{pmatrix} \ddot{\varphi}_1 \\ \ddot{\varphi}_2 \\ \ddot{\varphi}_3 \end{pmatrix}$$
$$+ \frac{ml^2}{6}\begin{pmatrix} 0 & 9\,s_{12} & 3\,s_{13} \\ -9\,s_{12} & 0 & 3\,s_{23} \\ -3\,s_{13} & -3\,s_{23} & 0 \end{pmatrix}\begin{pmatrix} \dot{\varphi}_1^2 \\ \dot{\varphi}_2^2 \\ \dot{\varphi}_3^2 \end{pmatrix}$$
$$+ \frac{mgl}{2}\begin{pmatrix} 5\,\cos\varphi_1 \\ 3\,\cos\varphi_2 \\ \cos\varphi_3 \end{pmatrix} = \begin{pmatrix} 1 & -1 \\ 0 & 1 \\ 0 & 0 \end{pmatrix}\begin{pmatrix} \tau_1 \\ \tau_2 \end{pmatrix} + \begin{pmatrix} \lambda_1 \\ \lambda_2 \\ \lambda_3 \end{pmatrix}R \quad (4)$$

Where, m and l denote the mass and length of the links, g is gravity acceleration, and for the sake of abbreviation it's taken $c_{ij} = \cos(\varphi_i - \varphi_j)$ and $s_{ij} = \sin(\varphi_i - \varphi_j)$.

Table1.Joint angles at the end of each sub-Motion

	θ_1^*	θ_2^*	θ_3^*	θ_4^*
start	0	0	0	0
at the end of M $_1$	0	$-\alpha$	$+\alpha$	$+\alpha$
at the end of M $_2$	$-\alpha$	$+\alpha$	$+\alpha$	$-\alpha$
at the end of M$_2$′	$+\alpha$	$+\alpha$	$-\alpha$	0
at the end of M$_1$′	0	0	0	0

Similarly, in sub-motion M_2 the equations of motion are:

$$\frac{m\,l^2}{6}\begin{pmatrix} 20 & 15\ c_{12} & 9\ c_{13} & 3\ c_{14} \\ 15\ c_{12} & 14 & 9\ c_{23} & 3\ c_{24} \\ 9\ c_{13} & 9\ c_{23} & 8 & 3\ c_{34} \\ 3\ c_{14} & 3\ c_{24} & 3\ c_{34} & 2 \end{pmatrix}\begin{pmatrix} \ddot{\varphi}_1 \\ \ddot{\varphi}_2 \\ \ddot{\varphi}_3 \\ \ddot{\varphi}_4 \end{pmatrix}$$

$$+\frac{m\,l^2}{6}\begin{pmatrix} 0 & 15\ s_{12} & 9\ s_{13} & 3\ s_{14} \\ -15\ s_{12} & 0 & 9\ s_{23} & 3\ s_{24} \\ -9\ s_{13} & -9\ s_{23} & 0 & 3\ s_{34} \\ -3\ s_{14} & -3\ s_{24} & -3\ s_{34} & 0 \end{pmatrix}\begin{pmatrix} \dot{\varphi}_1^2 \\ \dot{\varphi}_2^2 \\ \dot{\varphi}_3^2 \\ \dot{\varphi}_4^2 \end{pmatrix} \qquad (5)$$

$$+\frac{m\,g\,l}{2}\begin{pmatrix} 7\ \cos\varphi_1 \\ 5\ \cos\varphi_2 \\ 3\ \cos\varphi_3 \\ \cos\varphi_4 \end{pmatrix} = \begin{pmatrix} 1 & -1 & 0 \\ 0 & 1 & -1 \\ 0 & 0 & 1 \\ 0 & 0 & 0 \end{pmatrix}\begin{pmatrix} \tau_1 \\ \tau_2 \\ \tau_3 \end{pmatrix} + \begin{pmatrix} \lambda_1 \\ \lambda_2 \\ \lambda_3 \\ \lambda_4 \end{pmatrix}R$$

Since either head or tail link is connected with the ground, a frictional reaction force arises that by assuming the Coulomb friction model and utilizing the Lagrange's multipliers method with regarding the constraint equation, the normal component of reaction force, i.e. R, can be calculated from the last row of the matrix-form equations (4) or (5), respectively given for sub-motions M_1 and M_2, in which we should substitute:

$$\lambda_i = l_i\ \cos\phi_i + \mu\,\mathrm{sgn}\ \mathbf{v}_{tip}\cdot\hat{\mathbf{x}}\ \sin\phi_i \qquad (6)$$

Where, μ is the kinetic friction coefficient, and $\mathbf{v}_{tip}$ is the velocity vector of the tip of the last link in each sub-motion scuffing on the ground.

C. Cost Function Evaluation

As mentioned before, to shrink the weight of the actuators we must minimize the total torque required in each sub-motion. Minimizing the required torque should be achieved through generating the optimal joint trajectories. Hence, corresponding with a set of trajectories given for active joints, provided that those are able to satisfy the constraint equation (3) properly, solving the inverse dynamics yields the time history of torques in the active joints, and then a cost function can be evaluated as the below:

$$J = \psi(\Theta(t)) + \frac{1}{2}\int_0^{t_f}\left\|\boldsymbol{\tau}(\Theta(t))\right\|^2 dt \qquad (7)$$

where, the psi function evaluates the satisfaction of constraint, as a penalty function. Also, the integrated function is the norm of torque vector function consisted of torque values of the active joints. It is obvious that each one of these torques is a time function of all joint trajectories included in the vector Θ. The period of completing the sub-motions is t_f, too. Evaluating the integral term of the cost function called "dynamical effort" metric is done via discretization by a few samples of motion duration. Thus, it can be approximated by:

$$\frac{1}{2}\int_0^{t_f}\|\tau\|^2 dt \simeq \frac{1}{2}\sum_{i=1}^{n}\sum_{j=1}^{smp}\left(\frac{\tau_{i(j+1)} - \tau_{ij}}{2}\right)^2 \frac{t_f}{smp} \quad (8)$$

Where, *smp* is the number of samples.

3- Parametrization and Tragectory Generation

A.   B-spline Curves

The B-spline curves are typically specified in terms of a set of control points, let be P = { p_1 ,p_2,...,p_p}, and a knot vector, T = {t_1 ,...,t_k, t_{k+1} ,...,t_p, t_{p+1} ,...,t_{p+k}}.B-spline curves are a method for defining a sequence of degree *k*-1 Bézier curves that join geometrically together with C^{k-2} continuity, regardless of where the control points are placed. Unlike ordinary splines, B-spline curves do not interpolate the control points necessarily; however, the boundary points can be interpolated as well. Indeed, *k* extra knots are attached to the knot vector control the end conditions of the B-spline curve. By choosing a *k*-fold knot at each end of T, curve interpolates the end control points and

is tangent to the control polygon, formed by lines connecting the control points, at its end points. It is desired that each sub-motion is started from and finished at the rest. Hence, if the boundary points placed in the beginning and end of the P vector are also repeated, the slope of the trajectories will become zero at the boundary points; that is the velocities in the beginning and end of the driven joints are equal to zero. We choose the cubic B-spline curves, i.e. *k* = 4, in order to parameterize the trajectory of each active joint in terms of a set of control points as follows:

$$\theta(\mathbf{P},t) = \sum_{i=1}^{p} B_{i,k}(t)p_i \qquad (9)$$

Where $B_{i,k}(t)$ are the basic functions of order *k*, calculated by recurrence relations as follows:

$t_i < t < t_{i+1}$:
$$B_{i,k}(t) = \frac{t - t_i}{t_{i+k-1} - t_i} B_{i,k-1}(t)$$
$$+ \frac{t_{i+k} - t}{t_{i+k} - t_{i+1}} B_{i+1,k-1}(t), \qquad (10)$$
otherwise :
$$B_{i,k}(t) = 0,$$

Thus, the control points of theB-spline have only a local effect on thecurve geometry. In other words,for given any *t* in knot span [t_i,t_{i+k}] there are only *k* nonzero $B_{i,k}$ (*t*) in this knot span (i.e. $B_{i,k-1}$,..., $B_{i-k,k-1}$, $B_{i-(k-1),k-1}$). Moreover, it can be proved that:

$$\sum_{i=1}^{p} B_{i,k}(t) = 1 \qquad (11)$$

It gives a desirable property so that limits on displacements of joints can be imposed through limits on the control point p_i. This is, if one is constrained that $p_i < p_{max}$, then it follows that:

$$\theta(\mathbf{P}, t) \leq p_{\max} \quad \forall t \in [0, t_f] \qquad (12)$$

B. Parameterizing the Optimization Problem

In order to change the functional optimization problem (7) to an ordinary parameter optimization, we use B-spline curves to generate parametric trajectories. By considering the desired boundary condition in each sub-motion we have a parameter optimization problem of the form:

$$\begin{aligned} min : J(\mathbf{P}) &= \psi(\Theta(\mathbf{P})) + \frac{1}{2} \int_0^{t_f} \left\| \tau(\Theta(\mathbf{P})) \right\|^2 dt \\ sub.to : \ & p_{\min} \leq p_i \leq p_{\max}; \\ & \Theta(t = 0) = \Theta_0, \quad \Theta(t = t_f) = \Theta_f \\ & \dot{\Theta}(t = 0) = \dot{\Theta}(t = t_f) = 0 \end{aligned} \qquad (13)$$

4- Results and Descussion

Here, we examine different numbers of control points for constructing the B-spline curves. In terms of any considered number of CPs, a parametric optimization problem is solved and it obtains the optimal values of CPs by which a set of acceptable trajectories is achieved minimizing the required torque in the sub-motion. Because of dealing with a complicated problem arising from nonlinear equations of motion with many variables resulted from parameterization, we preferred to utilize a heuristic optimization method that was called the genetic algorithm (GA). The number of CPs examined was from 8 to 12. Indeed, we began from one point more than the number of CPs employed by [15], and continued until increasing a further point to CPs led to a decrease in the cost after optimization. Thus, in the case of sub-motion M_2 increasing the CPs consecutively resulted in a better solution having a lower cost, until 12 CPs. Thereafter this procedure ceased. Of course, maybe the optimization should be repeated by readjusting the mutation rate or the number of bits used in coding the variables into the chromosome string, in order to obtain the best result. These considerations beside the cost value and the values of non-boundary CPs constructing the optimal trajectories, obtained by GA, in terms of different number of CPs are listed in Table 2. In a similar way, the sub-motion M_1 was examined, too. However, we could obtain only two cases that added CPs resulted in decreasing the cost of sub-motion M_1 compared to reference [15]. These results are given by Table 4 (see appendix). In Figs. 3, 4, and 5 the achieved optimal trajectories, respectively, for active joints θ_1, θ_2, and θ_3 of sub-motion M_2, in terms of the number of CPs employed in constructing them, are depicted. The control points are considered for satisfying the boundary condition, and are also plotted so that they can show the span of knots in the each case. Similarly, in Figs. 6 and 7, respectively, the same information is depicted for active joints θ_1 and θ_2 of sub-motion M_1. Although the optimal trajectories achieved by increasing the number of CPs yield the lower cost, they show a bang-bang

like behavior that leads to more vibrations and earlier damages in mechanical devices. Therefore, it is reasonable that we have a tradeoff between an even trajectory and an efficient one. This seems that has taken place in the optimal trajectories of sub-motion M_2 generated by 11 CPs. Also, in the sub-motion M_1 the optimal trajectories generated by 4 CPs have an outstandingly more even form while losing a slight fitness versus less cost of those generated by 11 CPs.

Table2.The Optimal Solutions for Sub-motion M_1 Versus Variant Numbers of CPs[a]

	minimum cost obtained by GA versus 11 CPs for B-Splines	GA parameters	
		bit	*Mu*
	0.907 e-3 N^2m^2	6	0.005
Opt. CPs	θ_1: {13.36, 42.19, 33.75, 30.94, 27.42, 39.38, 35.16} θ_2: {-37.97, -32.34, -10.55, -11.25, -4.22, -29.53, -19.69}		
	minimum cost obtained by GA versus 8 CPs for B-Splines	GA parameters	
		bit	*Mu*
	0.924 e-3 N^2m^2	5	0.01
Opt. CPs	θ_1: {42.19, 42.19, 29.53, 39.38} θ_2: {-26.72, -32.34, -7.03, -28.13}		

The high accelerations in the beginning and end of motion are other matters that should be considered. Required torques in these durations should not cause motors to be saturated. Figs. 8 and 9 depict the time histories of the torques required by active joints in both sub-motions according to the optimal trajectories parameterized by 8 CPs in M_1 and 11 CPs in M_2, respectively. The maximum value of torque is 0.15 Nm and it is required at the head joint in the M_2, or at the tail joint in the M_2', correspondingly. Hence, the motors mounted at these joints must have the minimum torque capacity of 15 Nm. Two other motors can have a less torque capacity of about 7.5 Nm. These ranges of torque are almost respected if the other optimal trajectories with different number of CPs are used, too.

5- Conclusion

This paper was aimed at minimizing required torque of a crawling worm-like robot due to its gait design considerations. The optimization problem was solved via parameterization of joint trajectories, and consequently cost function, using cubic B-spline curves versus variant numbers of control points (CPs) in constructing them. The genetic algorithm was also utilized as the optimizer. It was obtained in both main sub-motions of locomotion mechanisms through which increasing the number of CPs could yield the optimal trajectories which had a considerable less value of dynamical effort introduced as the cost function. Compared to results reported by Ref. [15], we could achieve more optimal solutions for this problem. By considering the avoidance of bang-bang like trajectories, those were discarded while they were the most optimal solutions, and kept the trajectories having a

slight more cost, but were more even. Thus, the optimal trajectories with 11 CPs in sub-motion M2, and also with 8 CPs in sub-motion M1 were addressed as the optimums, by which the value of the cost versus results of Ref. [15] have become less about 25.6% and 15.6%, respectively, in M2 and M1.
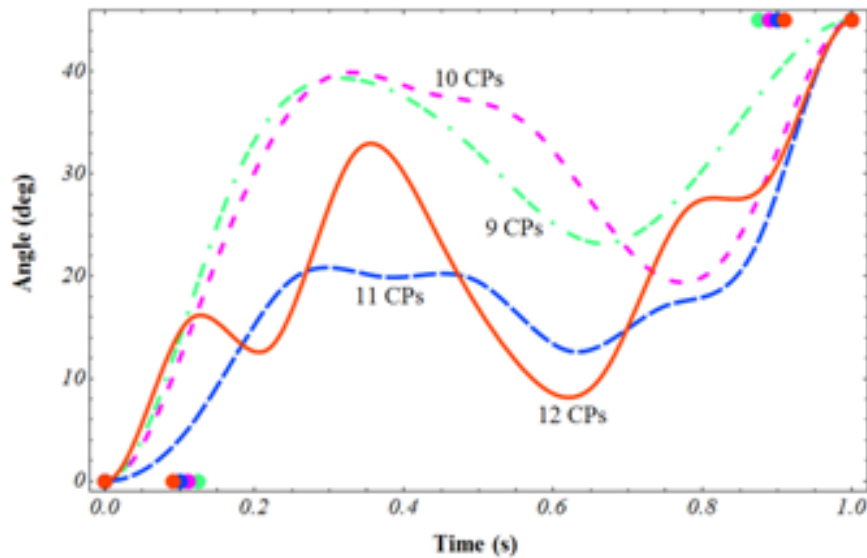

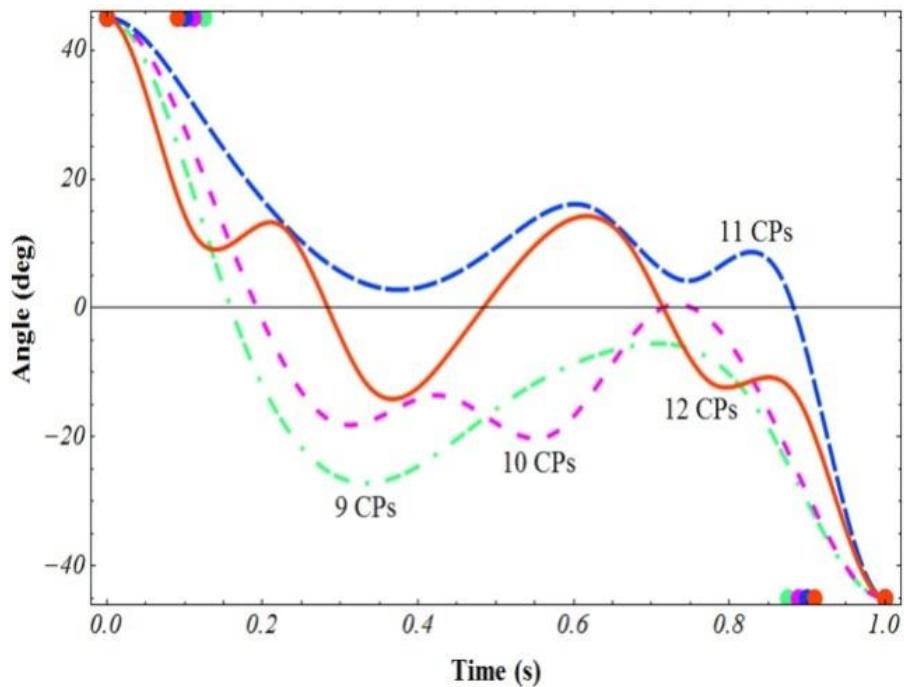**Fig.3.**Optimal trajectories for joint θ_1 of sub-motion M_2 vers number of CPs

Fig.4. Optimal trajectories for joint θ_2 of sub-motion M_2 vers number of CPs
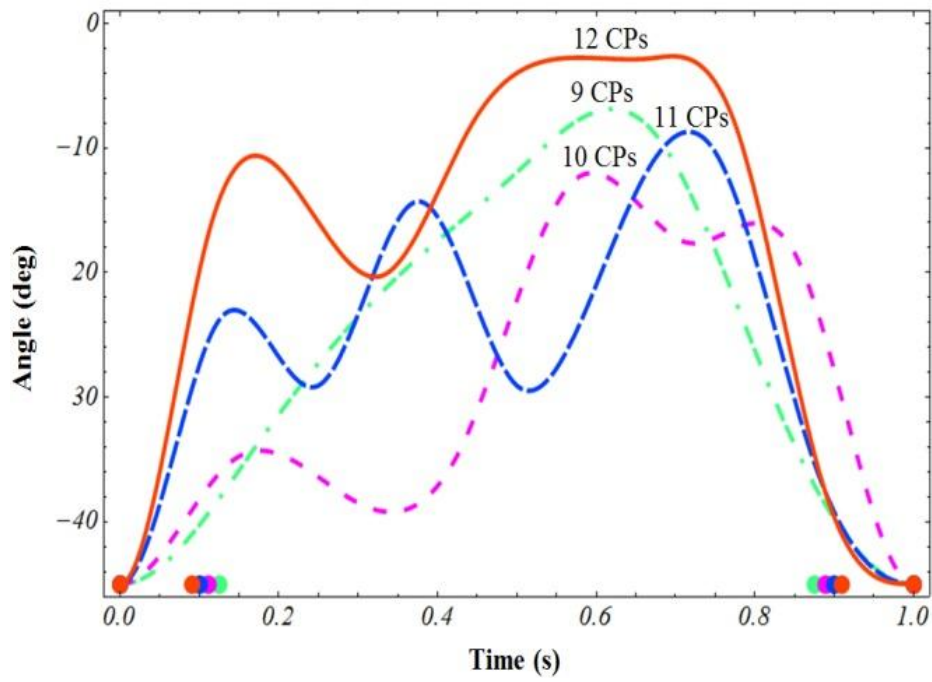
Fig.5. Optimal trajectories for joint θ_3 of sub-motion M_2 vers number of CPs
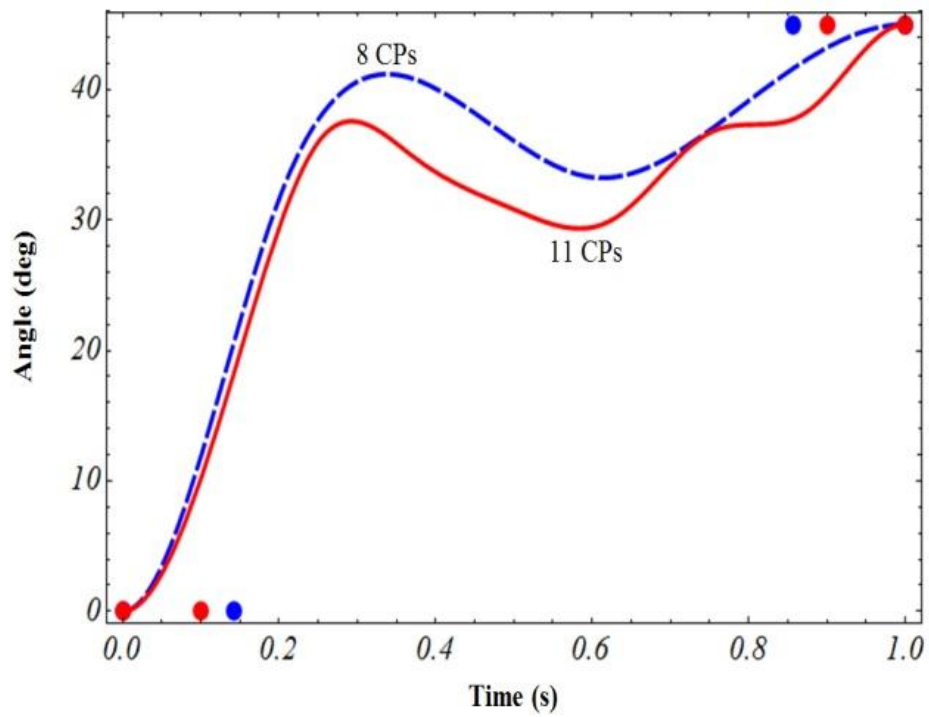
Fig.6. Optimal trajectories for joint θ_1 of sub-motion M_1 vers number of CPs
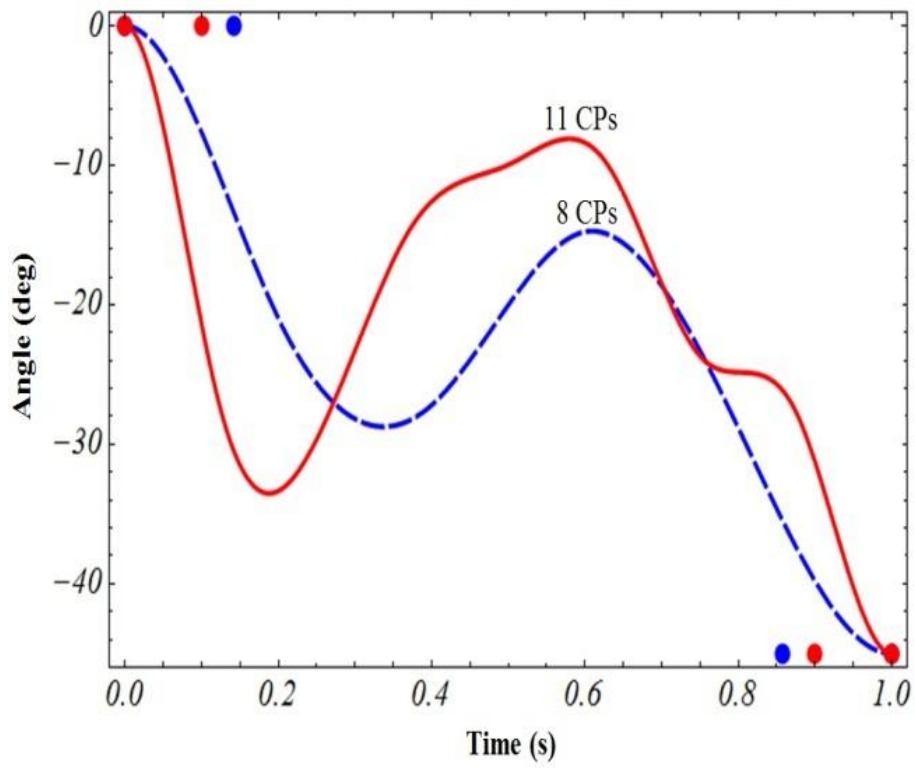
Fig.7. Optimal trajectories for joint θ_2 of sub-motion M_1 vers number of CPs
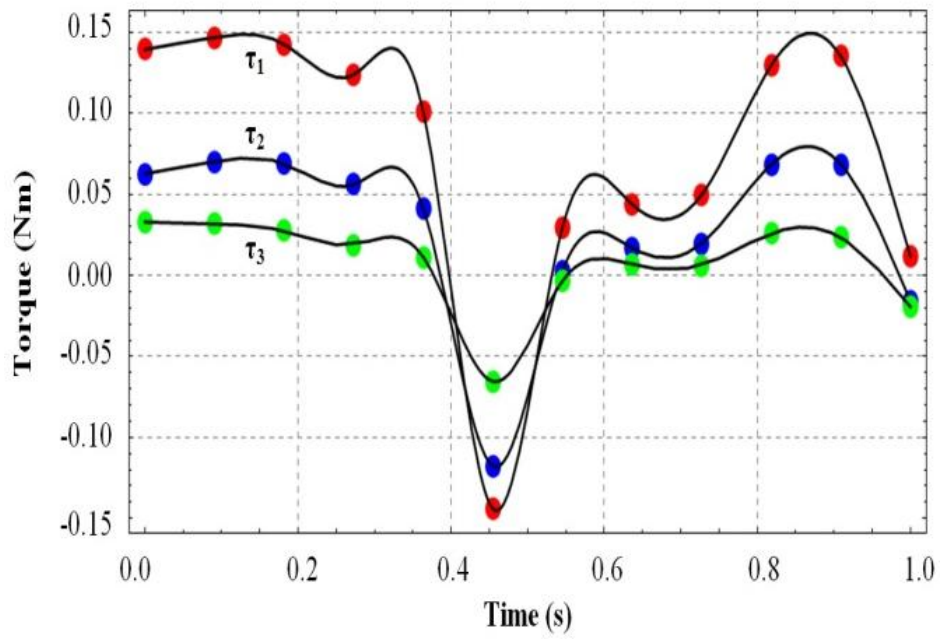

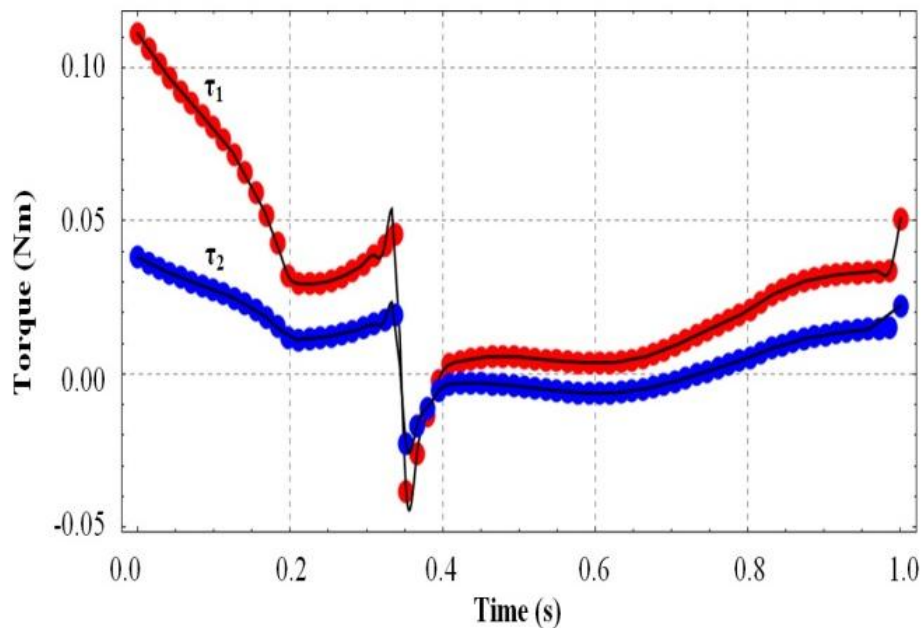**Fig.8.**Time histories of the torques required by active joints of M_2 (11 CPs)

Fig.9. Time histories of the torques required by active joints of M_1 (8 CPs)

References

[1] G. Li, W. Li, J. Zhang, H. Zhang,(2015). "Analysis and Design of Asymmetric Oscillation for Caterpillar-Like Locomotion," Journal of Bionic Engineering, vol. 12(2), pp. 190-203.

[2] R.H. Plaut, (2015). "Mathematical Model of Inchworm Locomotion," International Journal of Non-Linear Mechanics, in press.

[3] J. Lim, H. Park, J. An, Y-S. Hong, B. Kim, B-J. Yi, (2007). "One pneumatic line based inchworm-like micro robot for half-inch pipe inspection," Mechatronics, vol. 18(7), pp. 315-322.

[4] A. Goldenberg, M. Gryniewski, T. Campbell, (2010). "AARM: A robot arm for internal operations in nuclear reactors," IEEE Proc. of 1st Int. Conf. on Applied Robotics for the Power Industry, pp. 375-402, Montréal, Canada.

[5] P.R. Vundavilli, D.K. Pratihar, (2011). "Near-optimal gait generations of a two-legged robot on rough terrains using soft computing," Robotics and Computer-Integrated Manufacturing, vol. 27(3), pp. 521-530.

[6] J. Blair, T. Iwasaki, (2010). "Optimal Gaits for Mechanical Rectifier Systems," IEEE Trans. on Automatic Control, vol. 56(1), pp. 59-71.

[7] L. Biagiotti, C. Melchiorri, (2013). "Online Trajectory Planning and Filtering for Robotic Applications via B-spline Smoothing Filters," Proc. of the IEEE Int. Conf. on Intelligent Robots and Systems (IROS) , pp. 5668-5673, Tokyo, Japan..

[8] M. Kong, Ch. Ji, Zh.Chen, R. Li, (2013). "Smooth and Near Time-optimal Trajectory Planning of Robotic Manipulator with Smooth Constraint based on Cubic B-spline," Proc. of the IEEE Int. Conf. on Robotics and Biomimetics, pp. 2328-2333, Shenzhen, China.

[9] J.C. Restrepo, J. Villegas, A. Arias, S. Serna, C. Madrigal, (2012). "Trajectory Generation for a Robotic in a Robocup Test Scenery using Kalman Filter and B-Spline Curves," XVII Simposio de Tratamiento de Señales, Imágenes Y Visión Artificial, pp. 110-115, Antioquia.

[10] H. Kang, B. An, F.C. Park, (2010). "A Switching Formula for Optimal Gait Transitions," Proc. of

the IEEE Int. Conf. on Robotics and Biomimetics, pp. 30-35, Tianjin, China.

[11] J.D. Caigny, B. Demeulenaere, J. Swevers, J. D. Schutter, (2007). "Optimal Design of Spline-Based Feedforward for Trajectory Tracking," IEEE Proc. of the American Control Conference, pp. 4524-4529, New York, USA.

[12] K. Yang, (2013). "An Efficient Spline-based RRT Path Planner for Non-Holonomic Robots in Cluttered Environments," Proc. of the IEEE Int. Conf. on Unmanned Aircraft Systems , pp. 288-297, Atlanta, GA.

[13] W. Zhang, T. Inanc, S. Ober-Blobaum, J.E. Marsden, (2008). "Optimal Trajectory Generation for a Glider in Time-Varying 2D Ocean Flows B-spline Model," Proc. of the IEEE Int. Conf. on Robotics and Automation, pp. 1083-1088, California, USA.

[14] S.MR.S. Noorani, A. Ghanbari, (2009). "Using PSO for finding the optimal trajectory in minimizing the consumed energy of a crawling robot," Proc. of 17th ISME Annual Int. Conf. on Mechanical Engineering, Tehran, Iran.

[15] A. Ghanbari, SMRS. Noorani, (2011). "Trajectory Planning in Design of a Crawling Gait for a Modular Robot Using Genetic Algorithm," Int. J. Advanced Robotic Systems, vol. 8(1), pp. 29-36.

[16] A. Ghanbari, A. Rostami, SMRS. Noorani, MMS. Fakhrabadi, (2008). "Modeling & Simulation of Inchworm Mode Locomotion," Lecture Notes in Computer Science, Springer, Berlin, vol. 5314, pp. 617-624.

[17] SMRS. Noorani, A. Ghanbari, (2011). "Explicit Dynamic Formulation for n-R Planar Manipulators with Frictional Interaction between End-effecter and Environment," Int. J. Advanced Robotic Systems, vol. 8(2), pp. 91-100.

Appendix

Table 3. Values of Physical Parameters used in Simulation

mass (m)	link length (l)	gait angle (α)	frictioncoef. (μ)	duration (t_f)
15 gr	0.14 m	45 deg	0.4	1 sec

34

Table.4. The Optimal Solutions for Sub-motion M_2 Versus Variant Numbers of CPs[b]

	minimum cost obtained by GA versus 12 CPs for B-Splines	GA parameters	
		bit	*Mu*
	3.404 e-3 N^2m^2	6	0.01
Opt. CPs	θ_1: {26.02, 2.81, 41.48, 23.20, 9.84, 4.92, 33.05, 21.80} θ_2: {-7.03, 26.72, -22.50, -7.03, 12.65, 18.28, -22.50, 1.41} θ_3: {-6.33, -11.95, -26.02, -4.92, -2.11, -3.52, -0.70, -45.00}		
	minimum cost obtained by GA versus 11 CPs for B-Splines	GA parameters	
		bit	*mu*
	4.038 e-3 N^2m^2	5	0.01
Opt. CPs	θ_1: {4.22, 23.91, 18.28, 22.50, 8.44, 19.69, 15.47} θ_2: {28.13, 8.44, 0.00, 8.44, 22.50, -5.63, 25.31} θ_3: {-9.84, -40.78, -1.41, -39.38, -15.47, -1.41, -40.78}		
	minimum cost obtained by GA versus 10 CPs for B-Splines	GA parameters	
		bit	*mu*
	4.985 e-3 N^2m^2	5	0.01
Opt. CPs	θ_1: {22.50, 43.59, 36.56, 37.97, 18.28, 18.28} θ_2: {14.06, -28.13, -5.63, -30.94, 11.25, -14.06} θ_3: {-29.53, -39.38, -40.78, -2.81, -23.91, -7.03}		
	minimum cost obtained by GA versus 9 CPs for B-Splines	GA parameters	
		bit	*mu*
	5.348 e-3 N^2m^2	6	0.005
Opt. CPs	θ_1: {36.56, 41.48, 33.05, 18.28, 33.05} θ_2: {-14.06, -33.75, -14.06, -4.22, -5.63} θ_3: {-33.75, -20.39, -12.66, -0.70, -34.45}		